Louise Moore, K., Barac, M., Brajković, M., Bailey, M., Siketić, Z. & Bogdanović Radović, I. (2019) Determination of Deposition Order of Toners, Inkjet Inks, and Blue Ballpoint Pen Combining MeV-Secondary Ion Mass Spectrometry and Particle Induced X-ray Emission. Analytical chemistry, 91 (20), 12997-13005 doi:10.1021/acs.analchem.9b03058. Accepted Manuscrpt

Determination of deposition order of toners, inkjet inks and blue ballpoint pen combining MeV Secondary Ion Mass Spectrometry and Particle Induced X-ray Emission

Katherine L. Moore[a,b], Marko Barac[a], Marko Brajković[a], Melanie Bailey[b], Zdravko Siketić[a], Iva Bogdanović Radović[a] *

[a] Laboratory for Ion Beam Interactions, Ruđer Bošković Institute, Bijenička 54, HR-10000 Zagreb, Croatia
[b] Department of Chemistry, University of Surrey, Guildford, Surrey, GU2 7XH, UK
* Corresponding author.
Email address: iva@irb.hr (I. Bogdanović Radović)

Abstract

Determination of the deposition order of different writing tools is very important for the forensic investigation of questioned documents. Here we present a novel application of two Ion Beam Analysis (IBA) techniques: Secondary Ion Mass Spectrometry using MeV ions (MeV-SIMS) and Particle Induced X-ray Emission (PIXE) to determine the deposition order of intersecting lines made of ballpoint pen ink, inkjet printer ink and laser printer toners. MeV-SIMS is an emerging mass spectrometry technique where incident heavy MeV ions are used to desorb secondary molecular ions from the uppermost layers of an organic sample. In contrast, PIXE provides information about sample elemental composition through characteristic X-ray spectra coming from greater depth. In the case of PIXE, the information depth depends on incident ion energy, sample matrix and self-absorption of X-rays on the way out from the sample to the X-ray detector. The measurements were carried out using heavy ion microprobe at the Ruđer Bošković Institute. Principal Component Analysis (PCA) was employed for image processing of the data. We will demonstrate that MeV-SIMS alone was successful to determine the deposition order of all intersections not involving inkjet printer ink. The fact that PIXE yields information from deeper layers was crucial to resolve cases where inkjet printer ink was included due to its adherence and penetration properties. This is the first time the different information depths of PIXE and MeV-SIMS have been exploited for a practical application. The use of both techniques, MeV-SIMS and PIXE allowed the correct determination of deposition order for four out of six pairs of samples.

Keywords:
MeV-SIMS, PIXE, heavy-ion microprobe, forensic document examination, intersecting lines, molecular imaging, elemental imaging

Introduction

Determination of the deposition order of different writing tools is important in forensic science in the case when questioned documents are analyzed. Although most of the official documents produced today are printed using one of the commercially available printers, signatures are applied using different types of pen. The ability to determine the sequencing of pen and toner lines could help forensic scientists spot forgeries, alterations as well as establish a deposition order in case of questioned documents. Despite the usefulness of a technique for this purpose, most research has focused on identifying the components of pen inks or on intersections involving two pens. Due to printers not being commercially available till more recent years, work involving printed lines is less common[1], but with the ever-growing use of digital technology, equally important to forensics.

The most recognized techniques for looking at intersecting lines of any kind in forensic daily work are optical methods [2 3 4]. Physical characteristics can be highlighted by varying light sources and angles giving indications of which line was written second. Optical methods have the benefit of being affordable and entirely non-destructive,

but they often struggle when the intersecting lines have similar colors. Optical methods do not provide any information on writing tool chemical composition. Also, there is an element of interpretation meaning the conclusion can vary between examiners.

Lines that cannot be distinguished by optical methods require the use of more sophisticated instruments. Newer techniques for analysis include Raman spectroscopy[5], atomic force microscopy (AFM)[6], attenuated total reflectance-Fourier transform infrared imaging (ATR-FTIR)[7] and scanning electron microscopy - energy dispersive spectroscopy (SEM-EDS)[8]. Each technique has its own benefits and limitations but still, there is no definitive way of distinguishing different writing tools at an intersection.

Time-of-flight secondary ion mass spectrometry (ToF-SIMS) is a highly sensitive surface technique that provides high lateral resolution information. It has already been applied for investigating the sequencing of inks and toners. In one study three different black inks were tested[9] and the technique successfully distinguished the inks from each other, but one of the three inks dominated all the intersections leading to incorrect deposition order determinations. Another paper looked at the intersections of various colored pen inks with successful results[10]. ToF-SIMS has also been applied to inks, toners and stamp inks in conjunction with ATR-FTIR[11 12]. Due to ToF-SIMS extended mass range and higher sensitivity, the intersections that could not be determined using ATR-FTIR were successfully determined using the ToF-SIMS instrument.

Secondary Ion Mass Spectrometry using MeV ions (MeV-SIMS) is a technique where secondary molecular ions are desorbed from the sample surface after the passage of MeV ions. As MeV ions interact with the surface layer only through electronic stopping, less fragmentation is expected than in the case of ToF-SIMS with keV ions. So far, this technique has been applied to determine the deposition order of blue ballpoint pen ink lines[13]. Six different blue ballpoint pens were used and deposition order for all combinations of them was determined with success. It has also shown success determining if a fingerprint is above or below ink lines[14 15 16] and identifying and imaging of different synthetic organic pigments[17].

Particle Induced X-ray Emission (PIXE) analysis has previously been relatively unused for order determination of intersecting lines because alone it provides very little information to distinguish depths. Furthermore, because it is not a surface technique, a lot of background from the bulk paper is present in spectra which interferes with the ink and toner line signals. However, it is frequently used for elemental analysis of pen samples and historical documents[18].

In the present work, the potential for applying MeV-SIMS and PIXE to intersecting ink/toner lines was investigated.

Experimental

Measurements were performed using the Ruđer Bošković Institute (RBI) heavy ion microprobe. MeV-SIMS measurements were performed using an attached MeV-SIMS setup with a Time-of-Flight spectrometer described in detail in Tadić et al.[19] MeV-SIMS measurements were performed prior to PIXE because we have previously shown that it was sufficient to determine the correct deposition order for all cases where blue ballpoint pens were involved, due to the technique's surface sensitivity[13] . Measurements were carried out under vacuum (10^{-6}-10^{-7} mbar) and 8 MeV Si^{4+} ions were employed for the analysis with a lateral beam resolution of approximately 5 × 5 µm. Smaller sample areas (100 × 100 µm) were scanned first, far from the intersection region to define the mass spectrum of each ink and toner. After that, the intersection region up to 1200 × 1200 µm was scanned for imaging. The beam current in pulsed mode was about 0.2 fA. Primary ion fluence corresponding to approximately 15 minutes of measurement for each sample was 2×10^7 ions/cm^2. A +5 kV voltage was applied to the sample holder to direct the secondary molecular ions towards the TOF extractor. Multi-Stop Time-to-Digital Converter (TDC) Data Acquisition System in the heavy ion deflection start mode was used with 100 µs between the ion pulses of 4 ns duration.

PIXE was employed on the same set of samples in the same microprobe chamber using 2 MeV proton beam with a lateral beam resolution of approximately 5 × 5 µm^2. The scanned intersection region was 800 × 800 µm^2 and the beam current was about 80 pA. Primary ion fluence corresponding to approximately 10 minutes of measurement for each sample was 4.6×10^{13} ions/cm^2. SPECTOR[18 20] software was used to control all parameters and data acquisition during the experiment. Basic spectra inspection was carried out using mMass[21]. Principal Component

Analysis (PCA) was employed on images using Matlab tool simsMVA[22] to enhance the contrast between different chemical compositions of each pixel. The manufacturers and models of each of the writing tools used in samples are presented in **Error! Reference source not found.**, Samples for the measurements were produced using one blue ballpoint pen, three different laser printers, and two different inkjet printers, to give a total of 12 samples.

Table 1. Writing tools manufacturers and models

Writing tool	Manufacturer	Model	Colour of ink
Ballpoint pen	HiText	Grip 901	Blue
Laser printer 1	HP	Laser Jet pro 400 colour MFP m475	Black
Laser printer 2	HP	Laser Jet p1606dn	Black
Laser printer 3	HP	Color Laser Jet 4600 hdn	Black
Inkjet printer 1	Canon	PIXMA ix6550	Black
Inkjet printer 2	HP	PHOTOSMART C5180 ALL-IN-ONE	Black

Each combination of one ink/toner above the other was made. The pen lines were all deposited by the same person maintaining a normal writing pressure. A section of the paper roughly 1 x 1 cm incorporating the intersection was cut using tweezers and scissors and mounted on a silicon wafer using double-sided carbon tape. A microscope photo was also taken of each sample to give a reference image. Given that the primary ion fluence for MeV-SIMS does not exceed the static limit, radiation damage to the samples is presumed to be negligible. Thus, it was assumed that the same samples could be reused for the PIXE measurements with no alterations necessary. It is worth noting that the static limit is a fluence of ions above which spectral differences are observed in MeV-SIMS spectra. Due to the novelty of this work, it is currently unknown whether working below the static limit is sufficient to also preserve the integrity of trace elements as imaged by PIXE. Not all the samples were necessarily imaged at the exact same spot as for MeV-SIMS, which provided some insight into the stability of PIXE images after MeV-SIMS irradiation for the first time. Figure 1 shows microscopic images of samples: a) laser toner 3 on inkjet ink 2, b) inkjet ink 2 on laser toner 3. Rectangles indicate MeV SIMS (red) and PIXE (green) approximate scan area. Corresponding MeV-SIMS mass and PIXE X-ray spectra of ballpoint pen ink, inkjet ink 2, laser toner 3 and plain paper are displayed in Figures 2 and 3, respectively. PIXE X-ray spectra of ballpoint pen ink did not yield any significant peaks that are different from the X-ray spectrum of the paper.

Figure 1. Microscopic images of samples: a) laser toner 3 on inkjet ink 2, b) inkjet ink 2 on laser toner 3. Red and green frame colors indicate MeV SIMS and PIXE approximate scan area, respectively.

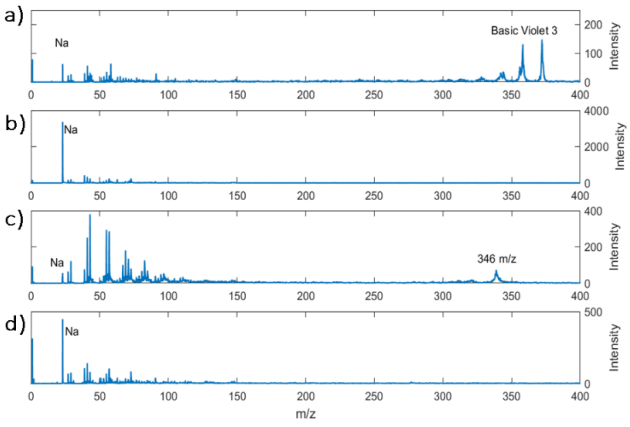

Figure 2. Individual mass spectra of a) ballpoint pen ink b) inkjet ink 2, c) laser toner 3, d) plain paper

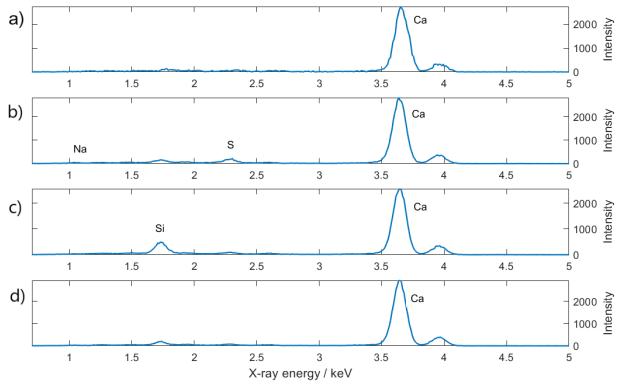

Figure 3. Individual PIXE spectra of a) ballpoint pen ink, b) inkjet ink 2, c) laser toner 3, d) plain paper

Results and Discussion

MeV-SIMS

All 12 samples were analyzed with MeV-SIMS. Because MeV-SIMS is a surface technique, it means that only molecules desorbed from the uppermost layer of the sample are detected and therefore the deposition order can be determined by looking at breaks in mapped image lines. The line deposited first should have a break while the line deposited second should be continuous. Also, the continuous line should have a thickness that matches that of the break.

PCA, a multivariate statistical analysis, was employed on all obtained hyperspectral images. In some cases, pixel binning of factor 2 was used due to a small number of counts per pixel, resulting in images of 64 x 64 pixels. Poisson scaling together with mean centering was applied in the pre-processing of images. PCA was performed via singular value deposition (SVD) with the use of sparse matrices. A predetermined number of 6 PC's for each case was set. Score maps of those PC's that represent the best contrast between writing tools or highlight a specific tool in an image are shown in Figures 4 to 9, with the results marked as correct or incorrect. Loading plots, showing significant mass peaks that contribute the most to the contrast of associated score map, are shown only in Figures 4 and 5 for simplicity (corresponding microscopic images of two cases are shown in Fig. 1). A discussion on the nature of the incorrect results is given later on.

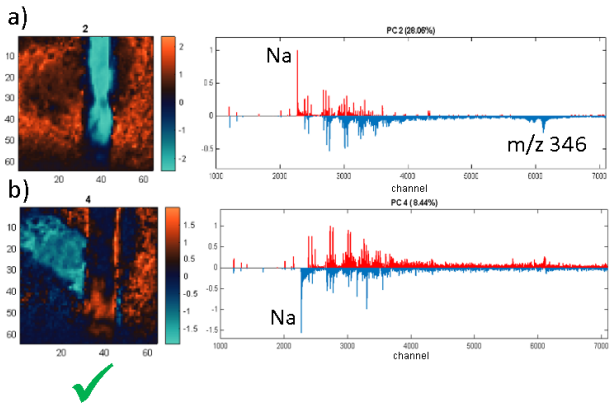

Figure 4. (MeV SIMS) **Laser toner 3 on inkjet ink 2**. a) PC2 (28.06%) map of laser toner 3 and the corresponding loading plot, b) PC4 (8.44%) map of inkjet ink 2 and the corresponding loading plot.

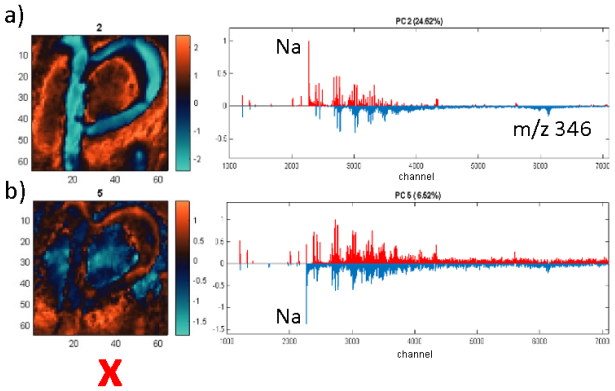

Figure 5. (MeV SIMS) **Inkjet ink 2 on laser toner 3**. a) PC2 (24.62%) map of laser toner 3 and the corresponding loading plot, b) PC5 (6.52%) map of inkjet ink 2 and the corresponding loading plot.

PCA analysis yielded good image contrast and mostly managed to distinguish between different writing tools based on the full mass spectra variance across pixels. It also detected major peaks contributing to those variances. Some peaks were already used in a simple preliminary RGB analysis prior to PCA, as they were easily recognized looking at the differences between spectra: lithium (m/z 7) for inkjet ink 1, sodium (m/z 23) for laser toner 1 and 2 and Basic Violet 3 (BV3) (m/z 372) for blue ballpoint pen ink. However, in the case of laser toners 1 and 2, PCA managed to detect some peaks in the lower mass region (m/z 55, 69 and 83) that have slightly higher intensities in laser toners 1 and 2 than in paper or inkjet ink 1. Similar to the inkjet ink 1, inkjet ink 2 is easily distinguishable from laser toner 3 using its most prominent sodium peak (m/z 23), but it does not contain any lithium. Laser toner 3 has an unknown peak at around m/z 346 and 648, and a lack of sodium which was used to identify it.

Out of the 6 pairs of samples, each pair comprised of two combinations in respect to deposition order of present writing tools, 2 pairs correctly showed a break in line deposited first - the pair containing ballpoint pen and laser toner 1 and the pair containing ballpoint pen and laser toner 2 (the latter is shown in Figures 9.a and 9.b). All the pairs involving inkjet ink caused problems when the inkjet ink was on top (Figure 5, Figures 6-8.a). Whether the inkjet line was deposited first or second, it always showed a break and the other line was always continuous, meaning that all interactions including inkjet ink could not be reliably established using MeV-SIMS alone. Because MeV-SIMS is a surface technique, this leads to a hypothesis that a) either the inkjet ink must be going below the other line into the paper or b) the inkjet ink was not adhering at the intersection at all. If it was not adhering, one may expect to see unabsorbed drops of ink. Unabsorbed drops of inkjet ink left on a layer of another writing tool at the intersection are usually noticed by microscopic methods, meaning it should also be possible for MeV-SIMS to detect them since they are present at the surface. However, in our case the inkjet ink 1 is characterized by a unique but low abundance of lithium, whereas the inkjet ink 2 is distinguished using different amounts of sodium with respect to the rest of the sample. In both cases, the attributes are not prominent or specific enough to significantly contribute to the overall mass spectrum in areas possibly containing drops. Consequently, it could be said that the detection limit is too low. Unfortunately, there were no higher-order PC's that highlighted a combination of laser toner and inkjet ink in the overlapping areas.

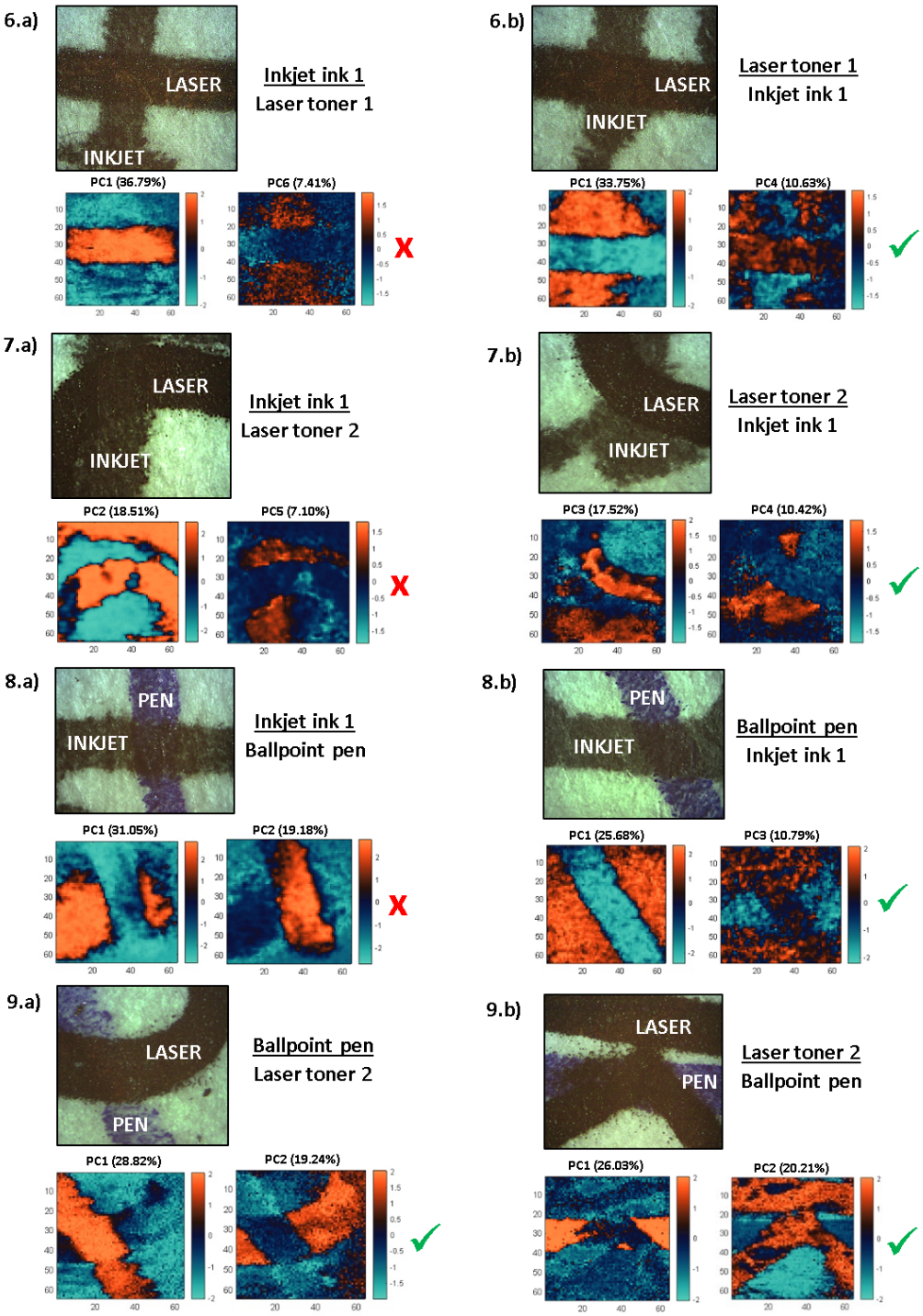

Figures 6 – 9. (MeV SIMS) Microscopic images of four pairs of samples and the corresponding PCA maps, highlighting differences between writing tools present in each sample; a) and b) denote two possible combinations of order. Samples involving combinations of a ballpoint pen and laser toner 1 are not shown because they yielded the same results as the samples involving combinations of a ballpoint pen and laser toner 2 (Fig. 9).

PIXE

In order to further investigate the behavior of inkjet inks interacting with other writing tools at the intersection, PIXE was used on the 8 remaining samples involving inkjet ink. The laser toner 1 and laser toner 2 with ballpoint pen line combinations were not analyzed using PIXE because these were adequately differentiated using solely MeV-SIMS, so no further analysis was necessary. As opposed to MeV-SIMS, PIXE is not surface sensitive and it gives

information from larger depths requiring only that the characteristic X-rays emitted from the sample are energetic enough to leave the sample and reach the X-ray detector.

PCA analysis of PIXE maps gave a clearer explanation for some of the cases. The line belonging to the inkjet ink will appear continuous at the intersection in two cases, the first is when the inkjet ink was deposited first, and the second when the inkjet ink is deposited second but is penetrating through the layer of the other writing tool (laser toner or ballpoint pen). The line belonging to the inkjet ink will have a break at the intersection only in case when it is deposited second and when it is not adhering to the already deposited writing tool.

PCA analysis of PIXE maps of a pair of samples involving laser toner 3 and inkjet ink 2 resulted in maps shown in Figures 10 and 11. Data was standardized (centered to have mean 0 and scaled to have standard deviation 1) prior to the analysis. Microscopic images of these samples, together with labeled writing tools, are shown in Figure 1.

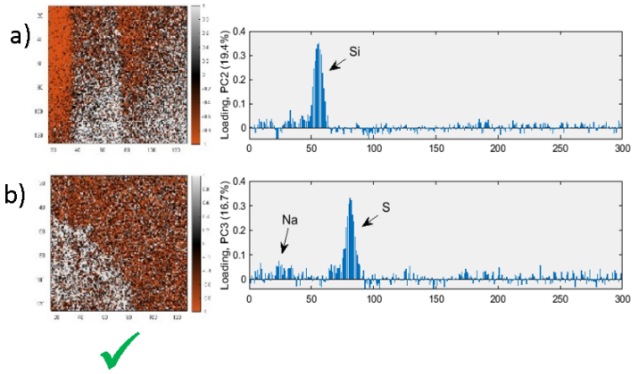

Figure 10. (PIXE) **Laser toner 3 on inkjet ink 2**. a) PC2 map of laser toner 3 and its loading plot, b) PC3 map of inkjet ink 2 and its loading plot.

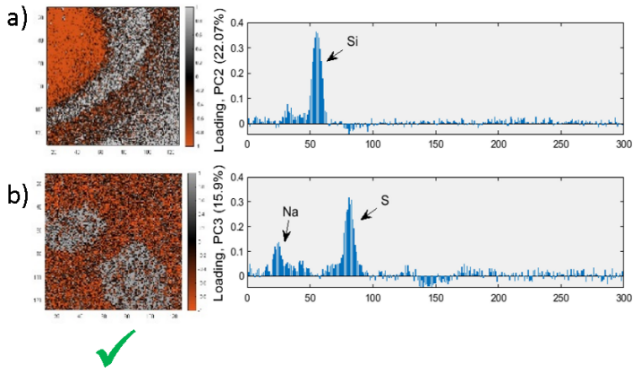

Figure 11. (PIXE) **Inkjet ink 2 on laser toner 3**. a) PC2 map of laser toner 3 and its loading plot, b) PC3 map of inkjet ink 2 and its loading plot.

Loading plots for PC1 in both cases represent the paper and are not shown here. It is clear from Fig. 10b that PIXE detected inkjet ink 2 from below laser toner 3 at the point of intersection, mainly from sulfur X-rays (sodium X-rays are mostly absorbed in the sample before they reach the surface, except in areas away from the intersection). But in the case when inkjet ink 2 was on top as in Fig. 11b, there is an evident break in the line at the point of intersection, which leads to a conclusion that there is no inkjet ink 2 deposited at all and that the substance below has prevented its absorption in the paper, in this case, laser toner 3. Also, there is a higher amount of sodium X-rays detected in respect to sulfur, which favors a hypothesis that there is no 'hidden' area of inkjet ink 2 under a layer of laser toner 3 which would absorb emitted low energy sodium X-rays. Similarly, score maps for the rest of the samples and their microscopic images are shown in Figures 12 – 14, with the results marked as correct or incorrect. Significant X-ray peak that contributed to highlighting of all laser toners is Si peak and the one highlighting all inkjet inks is S peak.

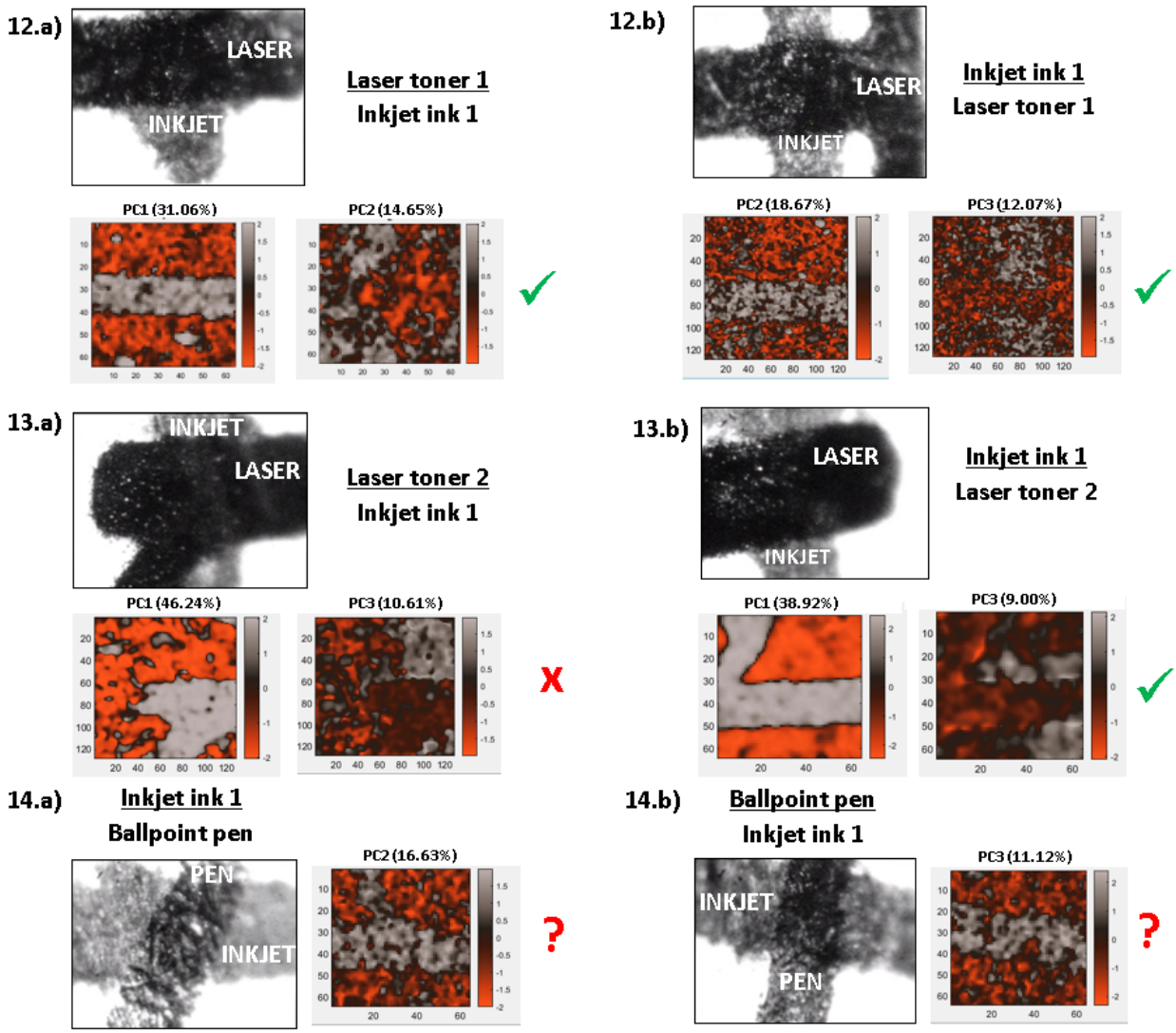

Figure 12 – 14. (PIXE) Microscopic images of three pairs of samples involving inkjet ink and the corresponding PCA maps highlighting differences between writing tools present in each sample. Figure 14 shows only PCA maps showing traces of inkjet ink because the ballpoint pen has not emitted any detectable X-rays.

Discussion

Error! Reference source not found. shows the complete collection of results obtained using both MeV-SIMS and PIXE. We successfully determined the deposition order of 4 out of the 6 pairs of samples. *Figure 15* shows a basic diagram depicting the different properties of the three writing tools, based on assumptions from this experiment. There is some variation between brands and types of printer. However, most commonly inkjet printers use water-based ink, ballpoint pen uses oil-based ink and laser printers use a wax-based toner. Inkjet ink tends to be mainly composed of water[23] meaning it penetrates deep into the paper and any remaining ink on the surface evaporates. Ballpoint pen ink, on the other hand, is oil-based, it has a relatively similar composition with the main difference being the choice of solvent and, as a result, the viscosity. It both penetrates into the paper and forms a membrane on top[24]. Laser printers work by melting a layer of resin to the surface of the paper[25].

MeV-SIMS indicated that the inkjet ink was not present on top of the intersection in the case where it should have been. Initially, it was proposed this may be because the inkjet ink was penetrating through the other inks deep into the paper. However, by using PIXE we were able to image the intersection below the surface and see this was not

the case. It was then proposed that perhaps the presence of the other ink between the inkjet ink and the paper was preventing it from adhering and penetrating into the paper entirely.

Table 2. Overall results of MeV SIMS and PIXE measurements of intersecting lines. Two pairs of cases remained unresolved.

	MeV SIMS results				MeV SIMS and PIXE combined results			
COMBINATION	**BREAK**	**CONTINUOUS**	**SUCCESS**	**RELIABLY DISTINGUISHABLE**	**BREAK**	**CONTINUOUS**	**SUCCESS**	**RELIABLY DISTINGUISHABLE**
Inkjet ink 1 / laser toner 1 Laser toner 1 / inkjet ink 1	Inkjet ink Inkjet ink	Laser Laser	X ✓	X	Inkjet ink -	Laser Inkjet ink, laser	✓ ✓	✓
Inkjet ink 1 / laser toner 2 Laser toner 2 / inkjet ink 1	Inkjet ink Inkjet ink	Laser Laser	X ✓	X	Inkjet ink Inkjet ink	Laser Laser	✓ X	X
Inkjet ink 1 / ballpoint pen Ballpoint pen / inkjet ink 1	Inkjet ink Inkjet ink	Ballpoint pen Ballpoint pen	X ✓	X	? ?	Inkjet ink, ? Inkjet ink, ?	X X	X
Ballpoint pen / laser toner 1 Laser toner 1 / ballpoint pen	Laser Ballpoint pen	Ballpoint pen Laser	✓ ✓	✓				
Ballpoint pen / laser toner 2 Laser toner 2 / ballpoint pen	Laser Ballpoint pen	Ballpoint pen Laser	✓ ✓	✓				
Inkjet ink 2 / laser toner 3 Laser toner 3 / inkjet ink 2	Inkjet ink Inkjet ink	Laser Laser	X ✓	X	Inkjet ink -	Laser Inkjet ink, laser	✓ ✓	✓

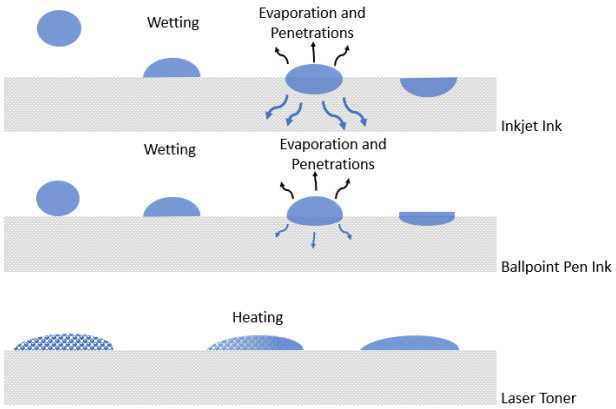

Figure 15 - Diagram of ink penetration and drying methods

By combining both MeV-SIMS and PIXE one can say that if there is a break in the inkjet line in both SIMS and PIXE then there is no ink at the intersection and conclude that it must have been prevented from adhering to the paper, therefore deposited second. However, two of the six pairs of samples were unsuccessfully distinguished even with both MeV-SIMS and PIXE. When mapped, the sample with laser printer 2 and inkjet ink 1 showed a break in the inkjet ink line whether it was above or below at the intersection. This is most likely due to the thickness of this particular laser toner and the amount of iron in its composition preventing the X-rays from the inkjet ink line reaching the detector. The other unsuccessful pair of samples was those containing the ballpoint pen and inkjet ink 1. The pen had no characteristic X-rays that could be used for mapping and distinguishing it from inkjet ink and paper. This means that the samples could not be mapped with PIXE and so were also unable to be distinguished.

Conclusions

The MeV-SIMS technique successfully determined the deposition order of intersections involving laser toners 1 and 2 and ballpoint pen. However, the sequencing of lines involving inkjet ink proved to be more challenging when the inkjet ink was on top. PIXE measurements of the problematic cases together with MeV-SIMS results contributed to understanding the behaviour of inkjet ink at the intersection and helped resolve the issue in most cases. Further analysis using more inkjet inks in combination with different writing tools is needed to establish the wider benefits of MeV SIMS and PIXE. Also, optimizing MeV SIMS setup to detect unabsorbed drops of inkjet ink left on the intersection could improve incorrect results and should be investigated.

MeV SIMS has proved to be a promising technique. Because of the limitations of chamber size, the technique as it is requires sampling (a sample needs to be cut and mounted on a sample holder in a vacuum chamber), which is

not ideal for forensic purposes. However, there is work underway for Ambient Pressure MeV SIMS (AP MeV SIMS)[26], which would remove the restraints of chamber size meaning the document would remain intact even after the analysis. On the other hand, AP MeV-SIMS is struggling with some difficulties which do not exist in vacuum MeV SIMS measurements, such as limitations in term of available heavy-ion beams due to the exit window thickness and more complex mass spectra due to the signal coming from the ambient. Also, the extraction of the secondary molecular ions from the sample to the mass spectrometer is currently inefficient.

Acknowledgments

K.L.M. acknowledges that the project was co-funded by the Erasmus+ program of the European Union. The European Commission's support for the production of this publication does not constitute an endorsement of the contents, which reflects the views only of the authors, and the Commission cannot be held responsible for any use which may be made of the information contained therein.
I.B.R. and Z.S. acknowledge support by the Croatian Centre of Excellence for Advanced Materials and Sensing devices research unit Ion Beam Physics and Technology, Ruđer Bošković Institute, Zagreb, Croatia, COST Action CA16101 (Multi-Foresee), and IAEA CRP F11021.
We also acknowledge Mrs. Andrijana Filko from the Forensic Science Center “Ivan Vučetić” for providing some of the samples and fruitful discussion.
M. Brajković acknowledges support by the Croatian Science Foundation project "Young Researchers’ Career Development Project - Training of Doctoral Students" co-financed by the European Union, Operational Program “Efficient Human Resources 2014-2020” and the ESF.
M. Bailey acknowledges EPSRC grant EP/R031118/1 : ion beam analysis for the 2020s and beyond : an integration of elemental mapping and omics for contributing her time to work on this project

References

(1) e Brito, L. v. R.; Martins, A. R.; Braz, A.; Chaves, A. B.; Braga, J. W.; Pimentel, M. F. *TrAC, Trends Anal. Chem.* **2017**, *94*, 54-69.
(2) Saini, K.; Kaur, R.; Sood, N. C. *Sci. Justice* **2009**, *49*, 286-291.
(3) Ozbek, N.; Braz, A.; López-López, M.; García-Ruiz, C. *Forensic Sci. Int.* **2014**, *234*, 39-44.
(4) Saini, K.; Kaur, R.; Sood, N. C. *Forensic Sci. Int.* **2009**, *193*, 14-20.
(5) de Souza Lins Borba, F.; Jawhari, T.; Honorato, R. S.; de Juan, A. *The Analyst* **2017**, *142*, 1106-1118.
(6) Kasas, S.; Khanmy-Vital, A.; Dietler, G. *Forensic Sci. Int.* **2001**, *119*, 290-298.
(7) Bojko, K.; Roux, C.; Reedy, B. J. *J. Forensic Sci.* **2008**, ???-???
(8) Kim, J.; Kim, M.; An, J.; Kim, Y. *J. Forensic Sci.* **2016**, *61*, 803-808.
(9) Goacher, R. E.; DiFonzo, L. G.; Lesko, K. C. *Anal. Chem.* **2016**, *89*, 759-766.
(10) He, A.; Karpuzov, D.; Xu, S. *Surf. Interface Anal.* **2006**, *38*, 854-858.
(11) Lee, J.; Nam, Y. S.; Min, J.; Lee, K.-B.; Lee, Y. *J. Forensic Sci.* **2016**, *61*, 815-822.
(12) Lee, J.; Kim, S. H.; Cho, Y.-J.; Nam, Y. S.; Lee, K.-B.; Lee, Y. *Surf. Interface Anal.* **2014**, *46*, 317-321.
(13) Malloy, M. C.; Radović, I. B.; Siketić, Z.; Jakšić, M. *Forensic Chem.* **2018**, *7*, 75-80.
(14) Bailey, M. J.; Jones, B. N.; Hinder, S.; Watts, J.; Bleay, S.; Webb, R. P. *Nucl. Instrum. Methods Phys. Res. B* **2010**, *268*, 1929-1932.
(15) Bright, N. J.; Webb, R. P.; Bleay, S.; Hinder, S.; Ward, N. I.; Watts, J. F.; Kirkby, K. J.; Bailey, M. J. *Anal. Chem.* **2012**, *84*, 4083-4087.
(16) Montalto, N. A.; Ojeda, J. J.; Jones, B. J. *Sci. Justice* **2013**, *53*, 2-7.
(17) Radović, I. B.; Siketić, Z.; Jembrih-Simbürger, D.; Marković, N.; Anghelone, M.; Stoytschew, V.; Jakšić, M. *Nucl. Instrum. Methods Phys. Res. B* **2017**, *406*, 296-301.
(18) Budnar, M.; Uršič, M.; Simčič, J.; Pelicon, P.; Kolar, J.; Šelih, V. S.; Strlič, M. *Nucl. Instrum. Methods Phys. Res. B* **2006**, *243*, 407-416.
(19) Tadić, T.; Radović, I. B.; Siketić, Z.; Cosic, D. D.; Skukan, N.; Jakšić, M.; Matsuo, J. *Nucl. Instrum. Methods Phys. Res. B* **2014**, *332*, 234-237.

(20) Bogovac, M.; Bogdanović, I.; Fazinić, S.; Jakšić, M.; Kukec, L.; Wilhelm, W. *Nucl. Instrum. Methods Phys. Res. B* **1994**, *89*, 219-222.
(21) Strohalm, M.; Hassman, M.; Košata, B.; Kodíček, M. *Rapid Commun. Mass Spectrom.* **2008**, *22*, 905-908.
(22) Trindade, G. F.; Abel, M.-L.; Watts, J. F. *Chemom. Intell. Lab. Syst.* **2018**, *182*, 180-187.
(23) Le, H. P. *J. Imaging Sci. Technol.* **1998**, *42*, 49 - 62.
(24) Kobilinsky, L. *Forensic Chemistry Handbook*; John Wiley & Sons, Inc., 2011.
(25) Li, B.; liang Ouyang, G.; nan Zhao, P. *J. Forensic Sci.* **2017**, *63*, 577-582.
(26) Matjačić, L.; Palitsin, V.; Grime, G. W.; Abdul-Karim, N.; Webb, R. P. *Nucl. Instrum. Methods Phys. Res. B* **2019**, *450*, 353-356.